SLAC-PUB-4751
October 1988
(I)

PERFORMANCE OF THE ELECTRONICS FOR THE LIQUID ARGON CALORIMETER SYSTEM OF THE SLC LARGE DETECTOR*

E. VELLA
University of Washington, Seattle, Washington 98195

I. ABT AND G. M. HALLER
Stanford Linear Accelerator Center, Stanford University, Stanford, California 94309

A. HONMA
University of Victoria, TRIUMF, Victoria BC, Canada V8W 2Y2

Abstract

Results of performance tests on electronics for the Liquid Argon Calorimeter (LAC) for the SLD experiment at SLAC are presented. The behavior of a sub-unit called a "tophat," which processes 720 detector signals, is described. The electronics consists of charge sensitive preamplifiers, analog memories, A/D converters, and associated control and readout circuitry. An internal charge injection system is used to calibrate the overall response of the devices. Linearity is better than 1% for 0–28 pC charge at the input of the amplifiers. Noise (expressed as equivalent input charge) is less than 3,000 electrons at a shaping time of 4 μs, with a slope of 2,600 e^-/pF. Crosstalk to adjacent channels is less than 0.5%. The power consumption at a duty cycle of 13% is 61 W.

1. Introduction

The SLC Large Detector (SLD) is a device for the study of electron-positron collisions at high energy. A major component of the detector is the Liquid Argon Calorimeter (LAC), which measures the energies of particles interacting in its lead-liquid argon volume. The measured signal is the ionization produced in the liquid argon by the incident particles and their secondary decay products. A more complete description of the calorimeter can be found in Ref. 1.

The front-end electronics for the LAC are located in 64 "tophats" which are mounted directly on flanges on the outside of the liquid argon cryostat. The cylindrical tophats measure 41 cm in diameter and 13 cm in height. The tophat and associated readout and control electronics are shown schematically in Fig. 1 and are described in more detail in Ref. 1.

Tophat operations are directed locally by a controller-board, which conducts the operations of the system in response to external commands and timing signals from a Fastbus Timing and Control Module.[2] Each tophat contains 15 daughter boards[1] to process the signals from the detector. One daughter board handles signals from 48 calorimeter towers, for a total of 720 towers per tophat. The daughter board data are digitized on an A/D-board and then transmitted serially via an optical fiber link to an external Fastbus processing module, the Calorimeter Data Module.[3]

Each daughter board contains several custom hybrids: six preamplifier hybrids, three preamplifier input protection hybrids, and three Calorimeter Data Unit hybrids (HCDU). The preamplifiers are low noise, charge sensitive amplifiers. An internal calibration system allows any individual channel or combination of channels to be calibrated by injecting a known charge at the preamplifier inputs. The HCDUs contain post-amplifier stages to provide both low and high gain (× 1 and × 8) for each input channel, 4 μs pulse shaping circuits, and a custom integrated circuit for separate baseline and peak signal sampling,

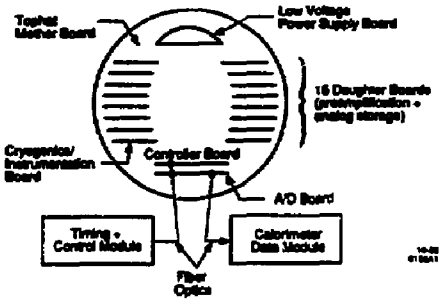

Fig. 1. Tophat electronics layout. Signals from 720 detector channels are preamplified, stored and then digitized on one tophat mounted directly on the detector.

analog storage, and parallel to serial output multiplexing. The dual range gain selection scheme, in combination with a 12 bit ADC, yields an overall dynamic range of 15 bits.

In the following sections, results of a series of performance tests on the tophat electronics are presented.

2. Linearity and Gain

The linearity and gain of the tophat electronics are measured with the internal calibration system. The calibration circuitry employs a 12 bit Digital-to-Analog Converter (DAC) with a full range of 2.5 V to generate a precision voltage which is switched onto calibration capacitors at each preamplifier input. The DAC is accurate to a few tenths of a millivolt, and the capacitors are laser trimmed to 8.4 pF ± 0.25 %. To eliminate baseline shifts and low frequency noise all channels are sampled both before and at the time the calibration pulse is applied. The digitized signals are sent via optical fiber from the tophat to external memory, where a peak minus baseline subtraction is performed as part of the analysis.

The gain calibration of the tophat electronics is achieved by pulsing all 720 channels at several different voltages. The response of each channel is fit to a straight line to determine the offset and gain. Typical results for a single channel are presented in Figs. 2–4. Figure 2a shows the low gain response of the system to calibration voltages from 250 mV to 2.5 V. An input voltage of 2.0 V represents a charge of 16.8 pC, the maximum charge deposited by a 50 GeV electromagnetic shower contained in a single tower. The high gain response of the system is shown in Figs. 3a and 4a for calibration voltages from 0 to 25 mV and 0 to 250 mV. A minimum ionizing particle traversing a small tower in the electromagnetic section of the calorimeter generates a charge of 24 fC or 150,000 electrons, corresponding

* Work supported by the Department of Energy, contract DE-AC03-76SF00515.

Presented at the Nuclear Science Symposium, Orlando, Florida, November 9–11, 1988

to a calibration voltage of 2.8 mV. The overall gain of the system is 1,400 ADC counts/8.4 pC at low gain, and a factor 7.6 greater at high gain. One ADC count at high gain thus represents about 5,000 electrons. Some adjustment of this gain is possible in the driver stage between the HCDU and the A/D board.

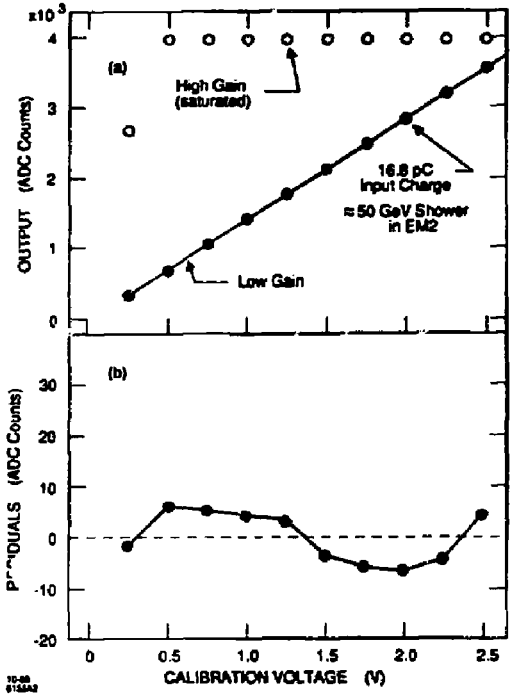

Fig. 2. a) Response of the electronics to large calibration signals. Charge is injected into the preamplifier via an 8.4 pF calibration capacitor. A 2 V pulse corresponds to the largest signal expected in a tower. The high gain response of the dual-range scheme is saturated. b) Residuals from a linear least-square fit of the low gain calibration points.

The tophat response is quite linear over the entire signal range, as can be seen from the plots of residuals (linear least-squares fit minus measured response), which are well under 1% at the high end and 1 ADC count at the low end of the scale (Figs. 2b, 3b, and 4b). In the final system, the calibration will be parametrized as a 16-point linear interpolation; this scheme should easily be able to correct the data to a few tenths of a percent.

3. Offsets

Both the peak and the baseline signals sit on "pedestals" of 100–200 ADC counts, provided to allow for negative signal fluctuations. The peak minus baseline subtraction removes these pedestals, but some non-zero offsets remain when no signal is input to the amplifiers. Large offsets, ranging from −20 to +120 ADC counts, are observed at high gain when calibrating the system with the DAC set to 0 V. The pattern of the offsets is similar on all daughter boards — groups of 8 or 16 similar channels (1 or 2 preamplifier hybrids or 1 HCDU hybrid) can clearly be distinguished. No large offsets are seen at low gain, but small offsets might be masked by the preamplifier noise. In normal physics

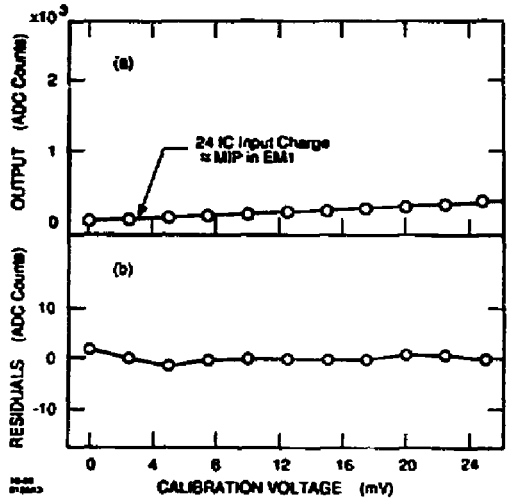

Fig. 3. a) Response of the electronics to small calibration signals. A 2.8 mV pulse corresponds to the smallest signal expected for a minimum ionizing particle (MIP). Only the high gain response of the dual-range scheme is shown. b) Residuals from a linear least-square fit of the high gain calibration points.

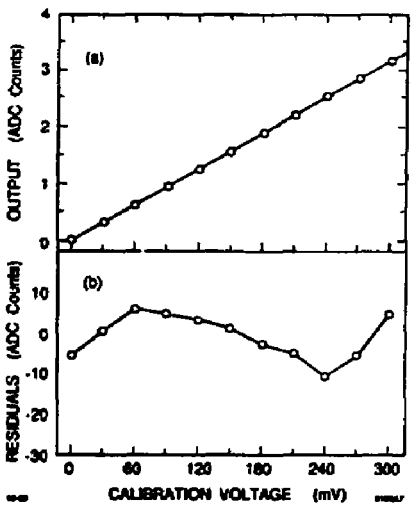

Fig. 4. a) Response of the electronics to calibration signals from 0 V to 250 mV (0 pC–2.1 pC). Only the high gain response of the dual-range scheme is shown. b) Residuals from a linear least-square fit of the high gain calibration points.

running, with the DAC not connected to the preamps, only small random offsets are observed, as can be seen in Fig. 5 (high gain response). It is suspected that the large calibration offsets are

due to stray charges at the preamplifier inputs induced by the switching circuitry. This circuitry connects the DAC to selected channels when running in calibration mode. Slight differences in transfer characteristics of analog storage cells in the HCDU are responsible for the small offsets obtained in normal running mode.

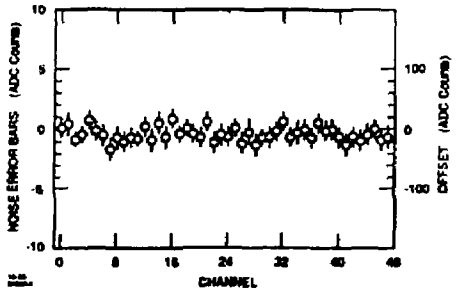

Fig. 5. Noise (error bars) and voltage offsets (points) of 48 signal channels on one daughter board. Shown is the high gain response after peak-baseline subtraction.

Large calibration offsets can easily be removed by starting every calibration run with the DAC set to 0 V. Blank events, taken out of time with respect to the beam crossing, can be used to subtract the small offsets seen in normal running mode.

4. Noise

Noise measurements are performed by pulsing the system repeatedly and calculating the width of the resulting output distributions. Noise results are included as error bars in Fig. 5. No difference in noise performance is seen between the calibration and normal physics modes. The observed noise is quite low, averaging roughly 0.7 ADC counts at high gain and 0.6 ADC counts at low gain. Referred to the preamplifier input, these noise values correspond to approximately 4,000 e^- and 28,000 e^- respectively.

The noise originating in the preamplifier and the HCDU hybrid is investigated in more detail by increasing the gain of the output stage in front of the A/D converters by a factor of 10. Digitization effects are then negligible. The noise with this setup is 4.1 ADC counts or 2,500 e^- at high gain and 2.7 ADC counts or 15,000 e^- at low gain. The noise at low gain is clearly dominated by the HCDU rather than the preamplifier and will never be significant in actual data taking. The noise at high gain is dominated by the preamplifier input stage.

Preamplifier protection hybrids, containing back-to-back diodes to ground, are connected to the preamplifier inputs to protect against high voltage discharges. Careful testing of a variety of diodes was necessary to select a model which does not seriously degrade the performance of the preamplifiers. The presence of the protection circuits increases the intrinsic preamplifier noise by about 10%.

The performance of the preamplifiers is strongly affected by tower capacitances connected at the input. Noise measurements with various external capacitors connected from the input to ground are shown in Fig. 6. Noise increases linearly with capacitance, with a slope of 2,600 e^-/nF, reaching a value of 18,000 e^- at a capacitance corresponding to a large tower in the hadronic section of the calorimeter.

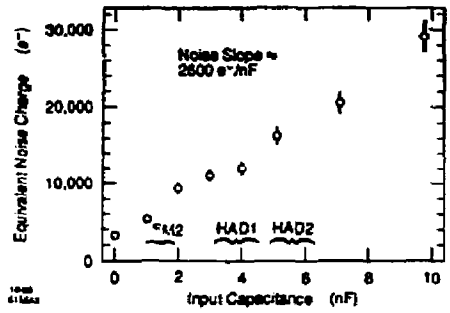

Fig. 6. Noise as a function of external capacitance at the preamplifier input. The capacitance ranges of various calorimeter towers are indicated (HAD: hadronic section, EM: electromagnetic section).

5. Crosstalk

The crosstalk of the system is measured by pulsing one tophat channel and recording the response of all 720 channels. Offsets are removed by subtracting an initial blank event from every measurement. The crosstalk matrix at high gain is shown in Fig. 7. Each row of the matrix corresponds to a particular pulsed channel; the entries along the row give the crosstalk fraction into other channels on the same daughter board (48 channels). All daughter boards on the tophat show the same crosstalk pattern within measurement errors.

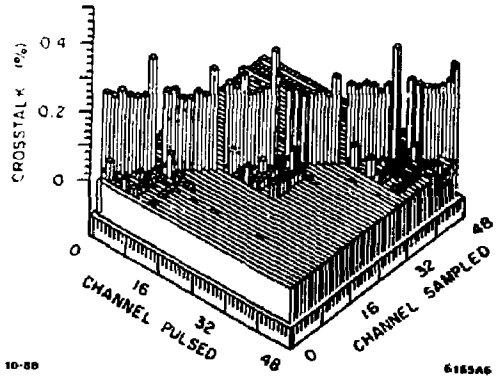

Fig. 7. Crosstalk. Response of 48 signal channels on one daughter board when one channel at a time is pulsed.

The crosstalk pattern is closely related to preamplifier and HCDU boundaries. Within the full crosstalk matrix, there are definite 8 × 8 sub-patterns corresponding to the six individual preamplifiers. There are also distinct 16 × 16 patterns related to the two back-to-back preamplifiers which share the same HCDU. Crosstalk outside a 16 × 16 block within a daughter board is completely negligible, as is crosstalk from one daughter board to another. Within a preamplifier, each channel except the last feeds through 0.3–0.4% to the next channel. Crosstalk to more distant channels is less than 0.1% everywhere. Note

that the crosstalk matrix is not symmetric — a large signal on channel n induces a small signal on channel $n+1$ but not on channel $n-1$.

Crosstalk in the actual calorimeter, with capacitive coupling between towers, will be considerably greater than the electronics crosstalk measured here. Further measurements are planned to investigate this crosstalk in a more realistic environment, with the goal of making crosstalk corrections to real data taken during normal running.

6. Temperature Dependence

The gain of the analog tophat electronics is somewhat temperature dependent, drifting by approximately 0.3%/°C. This temperature dependence is due to the transfer characteristic of the HCDU hybrid. Since the electronics is mounted on a large thermal mass in the detector, no short-term temperature changes are expected. The local temperature is monitored on each daughter board, and the electronics is recalibrated every few hours to correct for any long term drifts.

7. Power Consumption

The DC power consumption of a tophat is approximately 400 W, most of which goes to the preamplifiers. This power consumption, if not reduced, would lead to unacceptable heat generation in the experiment. The Stanford Linear Collider operates at a frequency of 120 Hz, which means that there is a period of 8.3 ms between beam-crossings; only 4 μs of this time is needed for the electronics (pulse shaping) to respond to an event. We take advantage of this situation to reduce the tophat power consumption by supplying the preamplifiers with pulsed power.

Tests show that power for the preamplifiers must be turned on 1 ms before beam-crossing to insure adequate stabilization of the preamplifier output levels. This is particularly important for cosmic ray data taking, where an event can occur at any time during a 100 μs gate. In order to enable both cosmic and normal physics runs at the same time, a total power-on time of 1.1 ms is chosen for the LAC front-end electronics. The duty factor for the preamplifiers is therefore 13% in normal physics, cosmic and calibration modes. At this duty cycle the tophat power consumption is reduced to 61 W.

References

[1] G. M. Haller, J. D. Fox and S. R. Smith, *The Liquid Argon Calorimeter System for the SLC Large Detector*, presented at this conference.

[2] Jack Hoeflich, University of Illinois, internal SLD document.

[3] L. Paffrath et al., *A General Purpose FASTBUS Data Acquisition Slave Module for SLD*, presented at this conference.

DISCLAIMER